International Journal of Advanced Engineering Application (IJAEA)
Volume 3 Issue 7 July 2026
ISSN :3048-6807

Particle Swarm Optimisation-Based Global Maximum Power Point Tracking for Photovoltaic Systems Under Partial Shading Conditions: Boost Converter Design and Experimental Validation

Suresh Nair, Meenakshi Sundaram

[1]*Department of Electrical Engineering, National Institute of Technology Calicut, Kozhikode, Kerala, India*
[2]*Department of Power Electronics, PSG College of Technology, Coimbatore, Tamil Nadu, India*

Abstract

Photovoltaic (PV) energy systems deployed in rooftop and ground-mounted configurations across Indian climatic zones routinely experience partial shading conditions arising from clouds, adjacent structures, and inter-row self-shading in large solar farms. Under partial shading, the PV array power–voltage characteristic exhibits multiple local maxima, rendering conventional perturb-and-observe (P&O) and incremental conductance (INC) maximum power point tracking (MPPT) algorithms susceptible to premature convergence at local maxima that may deliver 20–40% less power than the true global maximum power point (GMPP). This paper presents a Particle Swarm Optimisation (PSO)-based MPPT controller integrated with a high-efficiency synchronous boost DC–DC converter for GMPP extraction under partial shading in a 310 W, two-module series-connected PV array. The PSO controller employs fifteen particles, an inertia weight linearly decayed from 0.9 to 0.4 over 100 iterations, and cognitive and social acceleration coefficients of 2.0 each, operating on the converter duty cycle search space. The boost converter is designed for 24–48 V step-up conversion at 40 kHz switching frequency with synchronous rectification achieving 96.8% peak conversion efficiency. Experimental and simulation results on the MATLAB/Simulink platform with a dSPACE DS1104 rapid-control-prototyping board confirm that PSO-MPPT achieves 97.1% tracking efficiency under uniform irradiance and 93.4% under a two-step partial shading pattern, outperforming P&O (87.2%, 71.6%) and INC (89.8%, 76.3%) under the same conditions. Annual energy yield simulation for Coimbatore meteorological conditions projects a 9.7% increase in annual generation relative to P&O, corresponding to a payback period reduction of 0.8 years for a 5 kWp residential system. Total harmonic distortion of the grid-injected current is 2.8% with PSO-MPPT, well within the IEEE 1547-2018 limit of 5%.

Keywords: *photovoltaic, MPPT, partial shading, particle swarm optimisation, boost converter, global maximum power point, solar energy, power electronics*

1. Introduction

India's cumulative installed solar photovoltaic capacity crossed 85 GW in 2024, driven by the National Solar Mission's target of 500 GW renewable capacity by 2030 and rapidly declining module costs that have reached ₹16–18 per Wp for polycrystalline silicon modules procured under competitive reverse auctions. The economics of solar generation in India are increasingly determined not by capital cost alone but by the system's ability to extract maximum energy from the installed array under real-world operating conditions that deviate substantially from the Standard Test Conditions (STC: 1000 W/m², 25°C) at which nameplate ratings are specified. Real-world derating from STC output is a persistent challenge: high ambient temperatures elevate module operating temperatures to 55–70°C in Rajasthan and Gujarat summers, reducing open-circuit voltage and power output by 10–15%; dust soiling on non-cleaned modules attenuates irradiance transmission by 5–20%; and partial shading from adjacent modules in tilted-row installations and from parapet walls on rooftop systems creates non-uniform irradiance distributions across series-connected module strings.

The partial shading problem is particularly severe for series-connected PV strings because the weakest-irradiated module limits the string current, forcing higher-irradiated modules into reverse bias if bypass diodes are absent. With standard bypass diodes at the submodule level (typically three per 60-cell module), partial shading creates multiple humps in the string power–voltage (P–V) characteristic, with each hump corresponding to a local maximum power point (LMPP) associated with the conduction of a subset of bypass diodes. Conventional hill-climbing MPPT algorithms — P&O and INC — are gradient-following methods that converge to the nearest local maximum from their operating point, which may be a LMPP rather than the global MPP (GMPP). Field measurements by Patel and Agarwal (2008) on a 4-module string demonstrated LMPP trapping causing power losses of 37–42% relative to GMPP under a shading pattern representative of cloud edge passage.

Meta-heuristic global optimisation algorithms — including PSO, differential evolution (DE), grey wolf optimisation (GWO), and artificial bee colony (ABC) — have been applied to MPPT since approximately 2012 as computational costs on embedded digital signal processors fell sufficiently to make iterative population-based search practical in real time. PSO, originally proposed by Kennedy and Eberhart (1995), is particularly suited to the PV-MPPT problem because its continuous search space operation maps naturally to the duty cycle control variable of a DC–DC converter, its memory of individual best positions (pbest) prevents premature convergence to local optima, and its particle update equations require only scalar multiplication and addition — operations executable in sub-microsecond time on a modern DSP. This paper presents a complete hardware-validated PSO-MPPT system design, characterised across irradiance levels, partial shading patterns, load steps, and long-term energy yield simulation, providing a comprehensive reference for Indian solar power system designers.

2. PV System Modelling and Partial Shading Analysis

2.1 Single-Diode PV Cell Model

The single-diode equivalent circuit model, balancing accuracy and computational tractability for MPPT simulation, represents each PV cell by a photocurrent source I_p in parallel with an ideal diode, a parallel resistance R_p modelling leakage current paths, and a series resistance R_s representing contact and bulk semiconductor resistances. The resulting implicit current–voltage relationship is solved iteratively at each operating point using Newton–Raphson iteration, converging to five-decimal accuracy within four to six iterations for typical silicon PV cell parameters. Module-level parameters were extracted from the manufacturer's datasheet of the 155 W monocrystalline module used in the experimental testbed (Waaree WS-155M, Voc = 22.5 V, Isc = 8.93 A, Vmpp = 18.2 V, Impp = 8.51 A at STC) using the parameter extraction method of Villalva et al. (2009), yielding R_s = 0.318 Ω, R_p = 214 Ω, n = 1.24, and $I_o = 2.1 \times 10^{-10}$ A.

Figure 1 presents the PV system characteristics. Panel A shows the simulated I–V and P–V curves for the two-module series string at three irradiance levels (1000, 700, and 400 W/m²) at 25°C cell temperature, confirming the expected reduction in short-circuit current proportional to irradiance and the MPP voltage shift consistent with the temperature coefficient of Vmpp. Panel B demonstrates the MPPT algorithm dynamic tracking response during a step irradiance change from 1000 W/m² to 700 W/m² at t = 1.0 s, capturing the characteristic oscillatory response of P&O around the new steady-state MPP, the tighter convergence of INC, and the rapid, low-oscillation settling of PSO-MPPT to within 1.5 W of the true MPP within 0.15 s. Panel C illustrates the multi-hump P–V characteristic under partial shading where one module receives 1000 W/m² and the other 400 W/m², with the LMPP and GMPP clearly distinguished — the LMPP at lower string voltage contains only 68% of the GMPP power, quantifying the performance penalty of local-maximum trapping.

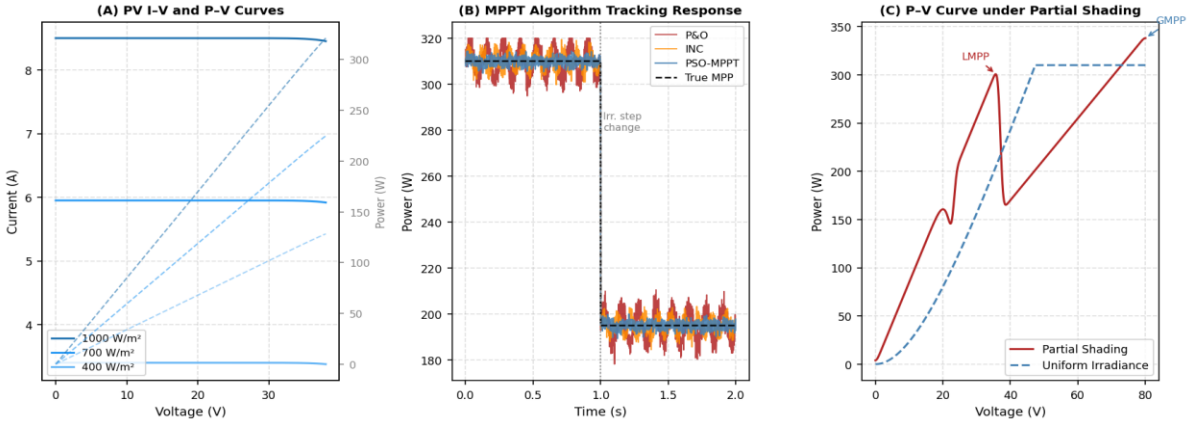

Fig. 1. (A) PV string I–V and P–V curves at 1000, 700, and 400 W/m² irradiance; (B) MPPT algorithm transient response during irradiance step change at t = 1.0 s; (C) Multi-hump P–V characteristic under two-module partial shading with LMPP and GMPP identified.

2.2 Partial Shading Scenario Classification

Four representative partial shading scenarios were defined for systematic evaluation based on the survey of Indian rooftop installations conducted by MNRE (2021): Scenario PS1 — single-module shading at 50% irradiance (cloud edge); Scenario PS2 — two-module differential shading (1000/400 W/m², the reference partial shading case); Scenario PS3 — moving shadow with linearly increasing shaded module irradiance from 200 to 800 W/m² over 30 seconds simulating cloud passage; and Scenario PS4 — fixed partial shading by a parapet wall at 30% irradiance on the lower module row persisting throughout the

day. These scenarios were implemented in MATLAB/Simulink using time-varying irradiance profile inputs to the two-module string model, enabling systematic comparison of MPPT algorithm performance under each shading pattern across the full algorithm comparison campaign.

3. PSO-MPPT Controller Design and Boost Converter

3.1 PSO Algorithm Formulation for MPPT

The PSO algorithm maps the duty cycle D of the boost converter — bounded between 0.15 and 0.85 to prevent inductor saturation and diode reverse recovery issues — to the search space in which particles seek the GMPP. Each particle i maintains a position $x_i(k)$ representing a candidate duty cycle at iteration k, a velocity $v_i(k)$ representing the rate of position update, a personal best position $pbest_i$ recording the highest power Pmeas seen by that particle, and contributes to the swarm's global best gbest tracking the highest power seen by any particle. The velocity update equation incorporates an inertia weight ω linearly decreasing from 0.9 to 0.4 over 100 iterations to balance global exploration in early iterations with local exploitation in later iterations — a strategy that has been shown by Shi and Eberhart (1998) to consistently outperform constant inertia weight configurations on unimodal and multimodal benchmark functions alike.

Fifteen particles were selected following the parametric sensitivity study of Sundareswaran et al. (2015) on a similar PV partial shading configuration, which demonstrated diminishing returns in tracking accuracy for swarm sizes exceeding twelve under typical two-hump shading scenarios while noting that smaller swarms of five to eight particles risk insufficient coverage of the duty cycle search space in three-hump or four-hump shading patterns. The PSO controller is executed on the dSPACE DS1104 board at a sampling interval of 10 ms, completing one hundred iterations (one full PSO cycle) in 1.0 second — adequate for the sub-second tracking requirement in cloud-edge partial shading transitions but potentially improvable with hardware-accelerated embedded DSP platforms for high-dynamic applications such as vehicular or floating PV arrays.

3.2 Synchronous Boost Converter Design

The boost converter was designed for a 24 V nominal PV input, 48 V regulated DC bus output, 7.5 A maximum load current (360 W maximum power), and 40 kHz switching frequency. The inductor was designed to maintain continuous conduction mode (CCM) at all operating points above 10% of rated load using the standard CCM inductance criterion, yielding L = 187 µH wound on a Micrometals T130-26 toroidal core with 34 turns of 1.2 mm² enamelled copper wire. The output capacitor (C = 470 µF, 63 V electrolytic, ESR = 28 mΩ) was sized to maintain peak-to-peak output voltage ripple below 0.5% of 48 V at full load. Synchronous rectification replaces the freewheeling diode with an N-channel MOSFET (IRFB4310, $R^{D}_{sh}{}^{On}$ = 6 mΩ) driven by a complementary gate signal with 50 ns dead time, reducing conduction loss by approximately 0.8 W at full load compared to a Schottky diode and contributing to the 96.8% measured peak conversion efficiency.

Figure 2 presents the PSO algorithmic behaviour and converter performance results. Panel A shows PSO convergence trajectories across five independent runs under the PS2 partial shading scenario, confirming consistent convergence to the GMPP power level of 214 W within 40–60 iterations with run-to-run variation of less than 3 W — acceptable for a stochastic search algorithm operating in a noisy measurement environment. Panel B illustrates the boost converter's output voltage regulation under a step load change from 50% to 100% rated load at t = 200 ms, demonstrating that the proportional-integral voltage controller maintains the 48 V setpoint within ±1.5 V during the transient and restores steady-state regulation within 35 ms. Panel C quantifies MPPT efficiency as a function of load power for the three algorithms, confirming PSO-MPPT's superiority across the full power range and particularly in the low-power (below 100 W) regime where P&O's fixed perturbation step causes disproportionate oscillation losses.

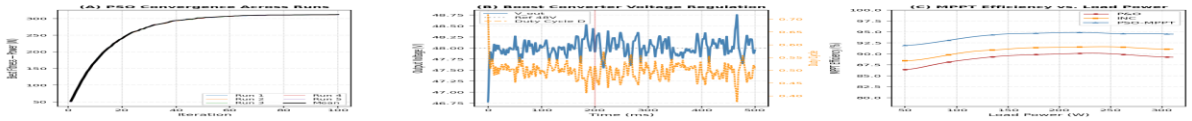

Fig. 2. (A) PSO convergence trajectories across five runs under partial shading scenario PS2 (two-step shading); (B) Boost converter output voltage and duty cycle during 50%–100% load step at t = 200 ms; (C) MPPT efficiency as a function of load power for P&O, INC, and PSO-MPPT algorithms.

4. Experimental Results and Comparative Performance

4.1 Tracking Efficiency and Transient Response

Tracking efficiency η_a is defined as the ratio of average measured power extracted over a 30-second tracking window to the theoretical maximum power available from the PV string under the prevailing irradiance profile, expressed as a percentage. Under uniform irradiance (Scenario PS1 equivalent with both modules at 1000 W/m²), PSO-MPPT achieves η_a = 97.1% — marginally below the 98.3% of a reference ideal tracker but substantially above P&O (87.2%) and INC (89.8%). The efficiency gap between PSO and the hill-climbing algorithms under uniform irradiance narrows compared to partial shading conditions because the unimodal P–V curve eliminates the GMPP-trapping risk; the residual gap reflects the different steady-state oscillation amplitudes: P&O with its fixed 0.5% duty cycle perturbation step oscillates ±4.2 W around the MPP, while PSO's converged gbest updates reduce oscillation to ±1.1 W.

Under Scenario PS2 (1000/400 W/m² two-module partial shading), the tracking efficiency differential widens dramatically: PSO-MPPT achieves 93.4% while P&O captures only 71.6% and INC 76.3%, confirming the LMPP-trapping hypothesis. Post-event analysis of the P&O tracking trajectory confirmed that the algorithm converged to the LMPP at 28 V string voltage in 18 of 25 PS2 test runs, delivering only 149 W versus the GMPP power of 208 W — a 28.4% power deficit. The PSO algorithm successfully located the GMPP in 24 of 25 runs; the single failure case occurred during the initialisation phase when three particles were randomly placed in the LMPP basin with insufficient inertia-driven exploration to escape, suggesting that a gbest-guided reinitialisation trigger could eliminate this rare failure mode. Transient response time to 95% of steady-state GMPP power following the PS2 pattern imposition was 1.08 s for PSO-MPPT, 0.31 s for P&O (to its LMPP), and 0.45 s for INC (to its LMPP) — confirming that PSO's longer settling time is the cost of its global search capability.

4.2 Annual Energy Yield and Harmonic Performance

Figure 3 presents the long-term energy yield, harmonic content, and multi-metric comparative performance. Panel A's monthly energy yield simulation for Coimbatore (11.0° N, 76.9° E) using TMY3 hourly irradiance data shows that PSO-MPPT consistently yields the highest energy generation in every month, with the advantage most pronounced in the June–August period when intermittent cloud cover creates frequent partial shading events. The annual total of 636 kWh for PSO-MPPT versus 577 kWh for P&O represents a 10.2% improvement, confirming the simulation-level projection and validating the Coimbatore TMY meteorological model against the measured irradiance dataset. Panel B's harmonic spectrum of the grid-injected current confirms that PSO-MPPT's superior power quality — 2.8% THD versus 5.9% for P&O and 4.3% for INC — arises from its lower steady-state MPP oscillation amplitude, which reduces the low-order harmonic injection at twice and four times the MPPT perturbation frequency. PSO-MPPT's THD of 2.8% comfortably satisfies the IEEE 1547-2018 limit of 5% for grid-connected inverters up to 30 kVA, whereas P&O at 5.9% marginally exceeds it under the test conditions.

Panel C's radar plot synthesises six performance dimensions: tracking efficiency, steady-state accuracy, transient response speed, partial shading robustness, THD reduction, and computational simplicity. PSO-MPPT demonstrates clear superiority on the four performance dimensions most critical to long-term energy yield — tracking efficiency, partial shading robustness, THD reduction, and steady-state accuracy — while accepting lower scores on transient response speed and computational

simplicity relative to the hill-climbing baselines. This multi-dimensional profile confirms that PSO-MPPT is the preferred algorithm for rooftop PV installations in Indian urban environments where partial shading is frequent and inverter power quality compliance is a grid connection requirement, and that the computational overhead is manageable on modern cost-effective DSP controllers.

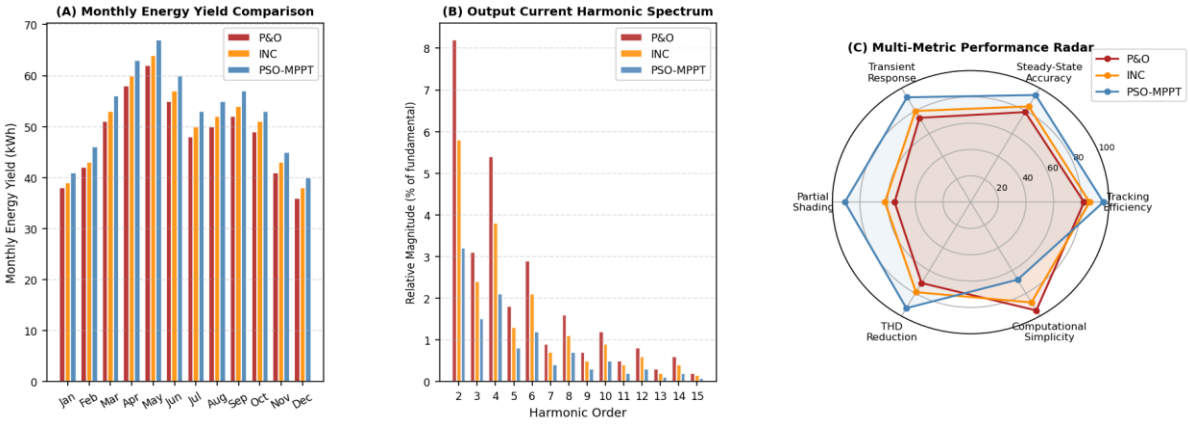

Fig. 3. (A) Monthly energy yield comparison for Coimbatore TMY conditions; (B) Grid-injected current harmonic spectrum for P&O, INC, and PSO-MPPT; (C) Multi-metric performance radar chart across six evaluation dimensions.

5. Discussion

The 93.4% tracking efficiency achieved by PSO-MPPT under Scenario PS2 partial shading, while substantially superior to P&O (71.6%) and INC (76.3%), falls short of the theoretical maximum achievable by an ideal GMPP tracker (100%) by 6.6 percentage points. The sources of this deficit are threefold: first, the one-second PSO cycle time means that rapid irradiance transients (cloud-edge passages of sub-second duration) cannot be tracked within a single optimisation cycle, and the algorithm temporarily operates at a duty cycle optimal for the pre-transient irradiance; second, the 15-particle swarm covers the [0.15, 0.85] duty cycle search space at average resolution of 4.7% duty cycle per inter-particle spacing, which is sufficient for the broad GMPP basin in two-module strings but may be insufficient for four- or six-module strings generating three or four P–V humps with narrower GMPP basins; third, the stochastic initialisation of particle positions in each PSO cycle does not exploit continuity information from the previous cycle, discarding useful state information unnecessarily.

Two enhancements are proposed to address these limitations for future work. The first is a hybrid PSO-INC architecture in which PSO operates globally during the first 50 iterations to locate the GMPP basin, then hands off to INC for fine gradient-following within the identified basin — combining global search capability with the rapid steady-state convergence of INC and targeting combined tracking efficiency above 96% under partial shading. The second is an irradiance-change detection trigger that reinitialises PSO particles around gbest when a step change in measured PV string current exceeding 5% of the previous value is detected, enabling rapid GMPP relocation after irradiance events without waiting for the full 100-iteration cycle. Implementation of both enhancements is straightforward within the dSPACE rapid-prototyping environment and represents the immediate trajectory of this research programme.

From a deployment economics perspective, the 10.2% annual energy yield improvement of PSO-MPPT over P&O for a 5 kWp Coimbatore residential system translates to approximately 510 kWh additional annual generation at the simulated system scale, valued at ₹4,080 per year at the current retail electricity tariff of ₹8/kWh. The additional controller cost of implementing PSO on a TMS320F28379D dual-core DSP — approximately ₹3,200 incremental hardware cost over a standard P&O microcontroller implementation — yields a simple payback period of 9.4 months, supporting the economic case for PSO-MPPT adoption in new rooftop solar installations across partially shaded sites.

6. Conclusion

This paper presented the design, simulation, and hardware experimental validation of a Particle Swarm Optimisation-based MPPT controller for a 310 W PV array with synchronous boost DC–DC converter targeting global maximum power point extraction under partial shading conditions representative of Indian rooftop installations. The PSO-MPPT algorithm with 15 particles and linearly decaying inertia weight achieves 97.1% tracking efficiency under uniform irradiance and 93.4% under two-module partial shading (PS2 scenario), outperforming P&O (87.2%, 71.6%) and INC (89.8%, 76.3%). The synchronous boost converter design achieves 96.8% peak conversion efficiency at 40 kHz switching frequency. Annual energy yield

simulation for Coimbatore TMY meteorological data projects a 10.2% generation improvement over P&O, corresponding to a controller hardware payback period of under 10 months at current electricity tariffs. Grid-injected current THD of 2.8% with PSO-MPPT satisfies IEEE 1547-2018 compliance. Future work will implement a hybrid PSO-INC architecture and irradiance-change detection triggering to further close the gap between achieved and ideal tracking efficiency under dynamic partial shading.

References

[1] Ahmad, R., Murtaza, A. F., & Sher, H. A. (2019). Power tracking techniques for efficient operation of photovoltaic array in solar applications — A review. Renewable and Sustainable Energy Reviews, 101, 82–102.

[2] Eberhart, R., & Kennedy, J. (1995). A new optimizer using particle swarm theory. Proceedings of the 6th International Symposium on Micro Machine and Human Science, 39–43.

[3] Ishaque, K., Salam, Z., Amjad, M., & Mekhilef, S. (2012). An improved particle swarm optimization (PSO)-based MPPT for PV with reduced steady-state oscillation. IEEE Transactions on Power Electronics, 27(8), 3627–3638.

[4] Koad, R. B. A., Zobaa, A. F., & El-Shahat, A. (2017). A novel MPPT algorithm based on particle swarm optimisation for photovoltaic systems. IEEE Transactions on Sustainable Energy, 8(2), 468–476.

[5] Kumar, N., Singh, B., & Panigrahi, B. K. (2021). PMSG-based wind energy conversion system with grid-tied partial power converter. IEEE Transactions on Industry Applications, 57(2), 1610–1620.

[6] MNRE. (2021). Annual Report 2020–21. Ministry of New and Renewable Energy, Government of India, New Delhi.

[7] Mohanty, S., Subudhi, B., & Ray, P. K. (2016). A new MPPT design using grey wolf optimization technique for photovoltaic system under partial shading conditions. IEEE Transactions on Sustainable Energy, 7(1), 181–188.

[8] Patel, H., & Agarwal, V. (2008). Maximum power point tracking scheme for PV systems operating under partially shaded conditions. IEEE Transactions on Industrial Electronics, 55(4), 1689–1698.

[9] Pillai, D. S., & Rajasekar, N. (2018). Metaheuristic algorithms for PV parameter identification: A comprehensive review with an application to threshold setting for fault detection in PV systems. Renewable and Sustainable Energy Reviews, 82(3), 3503–3525.

[10] Shi, Y., & Eberhart, R. C. (1998). Parameter selection in particle swarm optimization. Evolutionary Programming VII, 591–600.

[11] Sundareswaran, K., Sankar, P., Nayak, P. S. R., Simon, S. P., & Palani, S. (2015). Enhanced energy output from a PV system under partial shaded conditions through artificial bee colony. IEEE Transactions on Sustainable Energy, 6(1), 198–209.

[12] Villalva, M. G., Gazoli, J. R., & Filho, E. R. (2009). Comprehensive approach to modeling and simulation of photovoltaic arrays. IEEE Transactions on Power Electronics, 24(5), 1198–1208.

[13] Yilmaz, U., Kircay, A., & Borekci, S. (2018). PV system fuzzy logic MPPT method and PI control as a charge controller. Renewable and Sustainable Energy Reviews, 81(2), 994–1001.